

---

# Leak Rate, Ligament Rupture, and Burst Pressure Model Updates for Alloy 690 Thermally-Treated Steam Generator Tubes

---

Manuscript Completed: April, 2013  
Date Published September, 2018

Prepared by:  
Saurin Majumdar  
Argonne National Laboratory  
Illinois 60439  
USA

NRC Manager:  
Patrick Purtscher

## **Abstract**

This report summarizes the available flow stress and creep rupture properties data on thermally-treated Alloy 690 (690TT) and compares them with those of mill-annealed 600MA (600MA). The objective of this study was to evaluate analytically the leakage and rupture integrity performance of SG tubes made of 690TT during normal operation, design-basis accidents and severe accidents relative to 600MA. Equations for calculating ligament rupture pressure, unstable burst pressure, leakage area (needed for calculating leak rate), and time to creep rupture of 600MA steam generator (SG) tubes with cracks were developed and validated by tests and published by the author in earlier NUREG reports (NREG/CR-6575 and NUREG/CR-6774). Since failure data on 690TT tubes with notches are not available, the same set of equations were used to evaluate the performance of 690TT tubes with cracks relative to that of 600MA tubes with similar cracks during normal operation, design-basis accidents and severe accidents.



# Contents

Abstract.....	i
Contents.....	iii
Figures .....	v
Table .....	vii
Executive Summary .....	ix
Acknowledgments.....	xi
Acronyms and Abbreviations .....	xiii
1.0 Introduction .....	1
1.1 Objective .....	1
1.2 Background Information .....	1
1.2.1 Normal Operation and Design-Basis Accidents .....	1
1.2.2 Severe Accidents.....	4
2. Material Properties .....	5
2.1 Tensile Strengths of 600MA and 690TT.....	5
2.2 Creep Rupture Times of 600MA and 690TT .....	5
3. Experimental Basis for Ligament Rupture Pressure, Leak Rate and Unstable Burst Pressure Correlations for SG Tubes with Cracks .....	5
3.1 RT Tests.....	5
3.1.1 Ligament Rupture and Unstable Burst Pressures .....	5
3.1.2 Leak Rates .....	5
3.2 Severe Accident Tests .....	6
4. Comparison of Ligament Rupture and Burst Pressures and Leak Rates of 600MA and 690 SG Tubes.....	9
4.1 Normal Operation and Design-Basis Accidents .....	9
4.1.1 Ligament Rupture and Burst Pressures .....	9
4.1.2 Leak Rate .....	9
4.2 Severe Accidents .....	9
4.2.1 Comparison of Times to Rupture of Alloys 600 and 690 SG Tubes.....	10
5. Conclusions.....	12
6. References.....	13



## Figures

Figure 1. Predicted crack opening areas by FEA (finite deformation) vs. those predicted by the Zahoor model of 12.7 mm (0.5 in.) long axial notch for yield stress values of 179 MPa (26 ksi), 234 MPa (34 ksi) and 296 MPa (43 ksi) .....	4
Figure 2. Larson-Miller plot for time to creep rupture of Alloy 600. ....	7
Figure 3. Creep rupture curves of Alloy 690. Dashed lines represent extrapolated data trends. ....	7
Figure 4. (a) Larson-Miller plot for Alloy 690 creep rupture time data and the (b) observed vs. predicted creep rupture times using the LMP. ....	8
Figure 5. Predicted vs. observed times to rupture of Alloy 690.....	9
Figure 6. Observed vs. predicted (a) ligament rupture and (b) unstable burst pressures for rectangular EDM notches in 600MA tubes.....	5
Figure 7. Comparison of calculated (solid line) vs. experimentally measured (symbols) leak rates at 20 °C for as-received and heat-treated 22 mm (0.875 in.) diameter 600MA tubes with (a) 25.4 mm (1 in.) and (b) 12.7 mm (0.5 in.) axial EDM notches. Cross symbols (x) in Figure 7a denote calculated leak rates using posttest measured crack opening areas. ....	6
Figure 8. Calculated and ANL simulation of (a) INEEL ramp and (b) EPRI ramp for high-temperature tests. ....	6
Figure 9. Observed vs. predicted (a) failure temperatures and (b) failure times for tests simulating severe accident transients. Tests were conducted on 19 mm (0.75 in.) as well as 22 mm (0.875 in.) diameter 600MA tubes. Four nominal flaw geometries, with axial lengths of 6 mm (0.25 in.), 25 mm (1 in.), and 50 mm (2 in.) and depths varying from 20 percent to 65 percent of wall thickness, were tested. ....	7
Figure 10. Variations of pressure differential and temperature with time in the hottest SG tubes during the base case scenario. ....	10

Figure 11. Variations of mean and  $\pm 95$  percent prediction limits of the times to rupture of (a) 600MA and (b) 690TT hottest SG tubes subjected to the base case severe accident transient..... 11

Figure. 12. Comparison of the mean times to rupture of 600MA and 690TT tubes subjected to the base case severe accident transient. .... 11

## **Table**

Table 1 600MA and 690TT Tube Strength Properties!	6
---	---





## Executive Summary

This report fulfills a milestone originally included in the TIP-4 task on leak rate, ligament rupture and burst pressure model updates for thermally-treated, Alloy 690 (690TT) SG tubes. The objective of this study is to evaluate analytically the leakage and rupture integrity performance of SG tubes made of 690TT relative to the performance of mill-annealed, Alloy 600 (600MA) tubes during normal operation, design-basis accidents and severe accidents. Equations for calculating ligament rupture pressure, unstable burst pressure, leakage area (needed for calculating leak rate) and time to creep rupture of 600MA SG tubes with cracks were developed and validated by tests and published by the author in earlier NUREG reports (NUREG/CR-6575 and NUREG/CR-6774). Since test data on 690TT tubes with flaws are not available, the same set of equations were used to evaluate the performance of 690TT tubes with cracks by replacing 600MA properties with 690TT properties.

Earlier studies had shown that, for a given tube and flaw geometry, the ligament rupture, leakage and burst properties of 600MA tubes during normal operation and design-basis accidents were controlled by the flow stress properties of the material. Therefore, the available flow stress properties data on 690TT were reviewed and compared with those of 600MA. The comparison showed that the room-temperature yield and ultimate tensile strength of 690TT fall between the  $\pm 95$  percent prediction limits of 600MA tensile strength data. Based on this observation, we can conclude that the rupture and leakage behavior of 690TT SG tubes during normal operation and design-basis accidents should be very similar to that of 600MA SG tubes.

Earlier studies had also shown that, for a given tube and flaw geometry, the time to rupture properties of 600MA SG tubes during severe accidents are controlled by the creep rupture properties of the tube material at high temperatures. Available creep rupture properties of 690TT were collected and the data were replotted on a Larson-Miller plot. Analyses on the basis of the Larson-Miller plot showed that the mean time to rupture of an 690TT tube subjected to the pressure-temperature transients of the hottest tube during the accident exceeded that of an 600MA tube by 200-400 s.



## **Acknowledgments**

The work was funded by the US Nuclear Regulatory Commission under JCN N6582 . Mr. Charles Harris was the NRC manager when this work was done; the report was finished with Dr. Patrick Purtscher as the project manager.



## Acronyms and Abbreviations

<b>ANL</b>	Argonne National Laboratory
<b>EDM</b>	Electro-discharge machining
<b>EPRI</b>	Electric Power Research Institute
<b>FEA</b>	Finite Element Analysis
<b>INL</b>	Idaho National Laboratory
<b>ISL</b>	Information Systems Laboratories
<b>LMP</b>	Larson-Miller Parameter
<b>MA</b>	Mill-annealed
<b>MSLB</b>	Main Steam Line Break
<b>NRC</b>	Nuclear Regulatory Commission
<b>P<sub>b</sub></b>	Burst pressure of unflawed tube
<b>P<sub>cr</sub></b>	Critical burst pressure
<b>PTW</b>	Part-throughwall
<b>RT</b>	Room temperature
<b>SG</b>	SG
<b>TIP-2</b>	NRC-sponsored tube integrity program
<b>TT</b>	Thermally-treated
<b>TW</b>	Throughwall



# 1.0 Introduction

## 1.1 Objective

The objective of this report is to analytically estimate and compare the structural and leakage integrity performance of 690TT tubes relative to that of 600MA SG tubes with flaws during normal operation, design-basis accident and severe accident conditions. The procedures and equations used were developed by ANL and validated by tests on 600MA tubes with flaws in the past. No tests were conducted by ANL on Alloy 690 tubes, with or without flaws.

## 1.2 Background Information

### 1.2.1 Normal Operation and Design-Basis Accidents

#### 1.2.1.1 Burst and Ligament Rupture Pressures

The critical pressures and crack sizes for the unstable burst of a thin-wall internally pressurized cylindrical shell with a single TW axial crack can be estimated by equations 1(a-e)<sup>1-2</sup>

$$p_{cr} = \frac{\bar{\sigma}h}{mR} = \frac{p_b}{m}, \dots\dots\dots(1a)$$

where:

$$\bar{\sigma} = \text{flow stress} = k(S_y + S_u) \text{ (with } k = 0.5 - 0.6), \dots\dots\dots(1b)$$

$S_y$  and  $S_u$  are the yield and ultimate tensile strengths, respectively,

$$m = 0.614 + 0.481\lambda + 0.386\exp(-1.25\lambda), \dots\dots\dots(1c)$$

$$\lambda = [12(1 - \nu^2)]^{\frac{1}{4}} \frac{c}{\sqrt{Rh}} = \frac{1.82c}{\sqrt{Rh}}, \dots\dots\dots(1d)$$

$$p_b = \frac{\bar{\sigma}h}{R} = \text{burst pressure of an unflawed virgin tubing}, \dots\dots\dots(1e)$$

$R$  and  $h$  are the mean radius and wall thickness of tube,  $\nu$  is the Poisson's ratio, and  $2c$  is the axial crack length.

A general failure criterion for predicting rupture of the crack tip ligament in a tube with a PTW crack can be expressed as follows:<sup>1-2</sup>

$$\sigma_{lig} = \bar{\sigma}, \dots\dots\dots(2a)$$

where  $\sigma_{lig}$  is the average ligament stress, which for the axial crack is given by



$$\sigma_{lig} = m_p \sigma , \dots\dots\dots(2b)$$

where  $m_p$  is the ligament stress magnification factor (which depends on the axial crack length and depth), and  $\sigma$  is the nominal hoop stress (calculated using the mean radius and thickness of the tube, including the sleeve, if any).

An expression for  $m_p$  of rectangular PTW axial cracks was presented in Ref. 1 and is reproduced below:

$$m_p = \frac{1 - \alpha \frac{a}{mh}}{1 - \frac{a}{h}} , \dots\dots\dots(3a)$$

$$\alpha = 1 + \beta \left( \frac{a}{h} \right)^2 \left( 1 - \frac{1}{m} \right), \dots\dots\dots(3b)$$

where  $\beta = 1$ , and  $a$  is crack depth.

Equations 1(a) and 2(a-b) can be used to show that the unstable burst pressure ( $P_{cr}$ ) and the ligament rupture pressure ( $P_{SC}$ ) are given by:

$$p_{cr} = \frac{\bar{\sigma}h}{mR} \dots\dots\dots(4a)$$

$$P_{sc} = \frac{\bar{\sigma}h}{m_p R} \dots\dots\dots(4b)$$

It is evident from Eqs. 4(a-b) that for a given tube geometry ( $R$  and  $h$ ) and crack size ( $a$  and  $c$ ), the unstable burst and ligament rupture pressures are controlled by the tube material flow stress  $\bar{\sigma}$ , which is determined by the yield and ultimate tensile strengths of the material (Eq. 1b).

If  $P_{cr} \geq P_{SC}$ , the crack remains stable after ligament rupture and increased pressure is needed to cause tube-burst. On the other hand, if  $P_{cr} < P_{SC}$ , the crack experiences unstable burst immediately after ligament rupture, provided the test system has sufficient pressure and leak rate capacity.

### 1.2.1.2 Leak Rate

We have used the orifice discharge formula successfully in the past to calculate the volumetric leak rate  $Q$ :<sup>1-2</sup>

$$Q = 0.6A \sqrt{\frac{2\Delta p}{\rho}} \dots\dots\dots(5a)$$

or, using conventional units,

$$Q = 180.2A \sqrt{\frac{\Delta p}{\rho}}, \dots\dots\dots(5b)$$

where A is the flaw opening area in square inches, Δp is the pressure differential across the tube wall in pounds per square inch (psi), and ρ is the density (1000 kg/m<sup>3</sup> [62.4 lb/ft<sup>3</sup>] at RT and 735 kg/m<sup>3</sup> [45.9 lb/ft<sup>3</sup>] at 282 °C). Prediction of leak rates require a knowledge of the crack opening area A, which is different from a typical circular orifice whose area does not change significantly with pressure.

The flaw/crack opening area can be obtained either by finite-element analysis or by empirical equations, such as Zahoor’s model.<sup>1-2</sup> The crack opening area for an axial crack in a thin-walled tube is given by Zahoor’s model as:

$$A = 2\pi c_e^2 V_o \sigma / E, \dots\dots\dots(6)$$

where

$$\sigma = \text{hoop stress} = \Delta p R / h,$$

Δp = differential pressure across tube wall,

E = Young’s modulus,

$$V_o = 1 + 0.64935 \lambda_e^2 - 8.9683 \times 10^{-3} \lambda_e^4 + 1.33873 \times 10^{-4} \lambda_e^6,$$

$$\lambda_e^2 = c_e^2 / Rh, \quad c_e = c \left[ 1 + \frac{F}{2} \left( \frac{\sigma}{S_y} \right)^2 \right],$$

$$F = 1 + 1.2987 \lambda^2 - 2.6905 \times 10^{-2} \lambda^4 + 5.3549 \times 10^{-4} \lambda^6,$$

$$\lambda^2 = c^2 / Rh, \text{ and}$$

c = crack half length.

The flaw opening area for an EDM notch can be estimated by adding the initial flaw area (= flaw length x flaw width) to the crack opening area given by Eq. 6. Flaw opening areas calculated by Eq. 6 (adjusted for initial flaw area) agree well with FEA (finite element analysis) results (Figure 1).

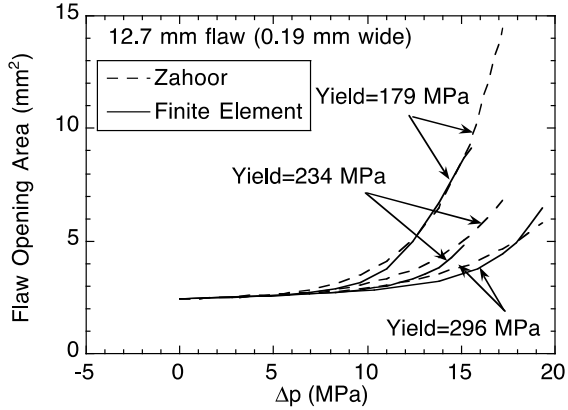


Figure 1. Predicted crack opening areas by FEA (finite deformation) vs. those predicted by the Zahoor model of 12.7 mm (0.5 in.) long axial notch for yield stress values of 179 MPa (26 ksi), 234 MPa (34 ksi) and 296 MPa (43 ksi)

It is evident from Eqs. 5-6 that for a given tube geometry (R and h) and crack size (2c), the leak rate at a given pressure is controlled by the tube material yield stress  $S_y$ .

### 1.2.2 Severe Accidents

Two models, a flow stress model and a creep rupture model, for predicting rupture of unflawed and flawed SG tubes during severe accidents were developed and reported in NUREG/CR-6575.<sup>3</sup> In the flow stress model, an assumption was made that rupture of the unflawed tube would occur when the hoop stress in the tube equals the flow stress of the tube material, i.e.,

$$\sigma = \bar{\sigma}(T) \dots\dots\dots(7)$$

where  $\sigma$  = hoop stress in the tube, T = tube temperature, and  $\bar{\sigma}$  = temperature-dependent (but strain rate-independent) flow stress of the tube material, which is assumed to be the average of the yield and the ultimate tensile strengths. An alternative, based on a creep rupture model, assumed that the unflawed tube would rupture when the following equation is satisfied:

$$\int_0^{t_f} \frac{dt}{t_R(T, \sigma)} = 1 \dots\dots\dots(8)$$

where  $t_R$  = stress and temperature-dependent time to rupture. The mean value of the time to rupture is usually represented by a Larson-Miller parameter (LMP),

$$LMP = (T+273)[C+\text{Log}_{10}(t_R)] \dots\dots\dots(9)$$

where T is in °C and C is a fitting parameter. Tests conducted on SG tubes with and without notches at high temperatures showed that the failure times and temperatures were predicted more accurately by using the creep rupture model than by the flow stress model.<sup>3</sup>

## **2. Material Properties**

### **2.1 Tensile Strengths of 600MA and 690TT**

A summary of the yield and ultimate strengths for one size tubing at both room temperature (RT) and at elevated temperature (650°F) are shown in Table 1 (from vendor database\*). The effects of heat-treatment (MA and TT) on the tensile properties of Alloys 600 and 690 were available only for 0.875 in. diameter tubes, but it is evident that both the RT and 650 °F tensile strength properties of the 690TT are within the scatter bounds of 600MA properties. Generally, the yield strengths at 650 °F are 20 percent lower and the ultimate tensile strengths at 650 °F are 10 percent lower than the respective values at RT.

### **2.2 Creep Rupture Times of 600MA and 690TT**

A large database on creep rupture properties of 600MA were collected and fitted to a Larson-Miller plot as part of the work reported in NUREG/CR-6575.<sup>3</sup> The plot is shown in Figure 2, which also includes the  $\pm 95$  percent prediction limits and the various equations that were used to fit the data.

We conducted a literature search on 690TT tube properties. We also obtained some literature from Mr. Charles Harris of NRC and Dr. Ali Azram of ISL. We collected creep rupture data for Alloy 690 from Ref. [4]. Although the specimens cited in this report were not thermally treated, their creep rupture time properties at high temperatures should be comparable to those of the thermally treated material. The above-cited reference does not give individual data points, but gives a series of rupture curves at nine different temperatures, which were digitized and are replotted here in Figure 3. The time to rupture curves are plotted at temperatures ranging from 900 to 2000 °F and for rupture times up to  $10^4$  hrs.

---

\* Personal Communication from R. Keating, Westinghouse to W. J. Shack, ANL, 2000.

Table 1 600MA and 690TT Tube Strength Properties<sup>†</sup>

<b>Mill-Annealed 600 Tubing</b>		
Temperature, °F	<b>RT</b>	<b>650°F</b>
<u>Yield Strength, <math>S_y</math>, ksi</u>		
Sample Mean, m	50.98	41.89
Standard Deviation, s	4.21	3.59
Lower Tolerance Limit, LTL	43.47	35.49
<u>Ultimate Strength, <math>S_u</math>, ksi</u>		
Sample Mean, m	99.96	95.67
Standard Deviation, s	3.61	3.42
Lower Tolerance Limit, LTL	93.52	89.57
<b>Thermally-Treated Alloy 690 Tubing</b>		
Temperature, °F	RT	650°F
<u>Yield Strength, <math>S_y</math>, ksi</u>		
Sample Mean, m	49.37	40.54
Standard Deviation, s	1.96	1.72
Lower Tolerance Limit, LTL	45.98	37.31
<u>Ultimate Strength, <math>S_u</math>, ksi</u>		
Sample Mean, m	105.27	95.31
Standard Deviation, s	2.04	2.04
Lower Tolerance Limit, LTL	101.73	91.38

<sup>†</sup> 7/8 inch Diameter by 0.050 inch

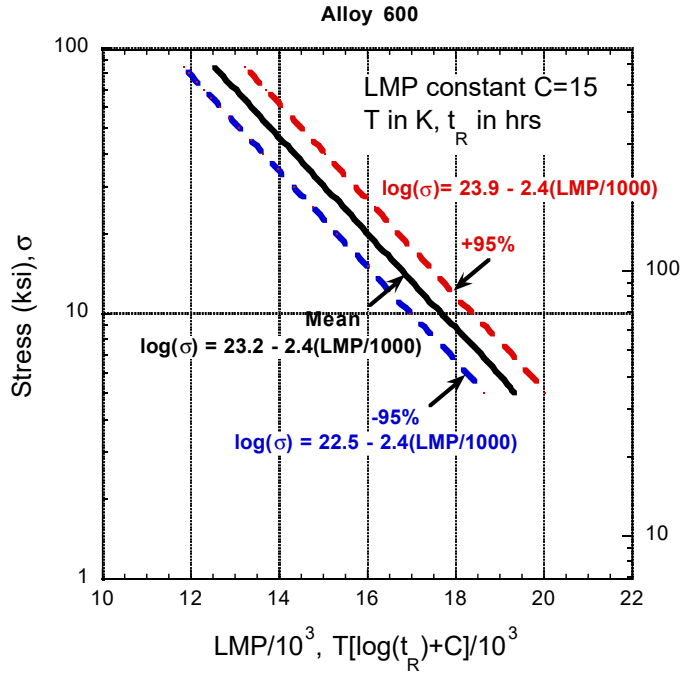


Figure 2. Larson-Miller plot for time to creep rupture of Alloy 600.

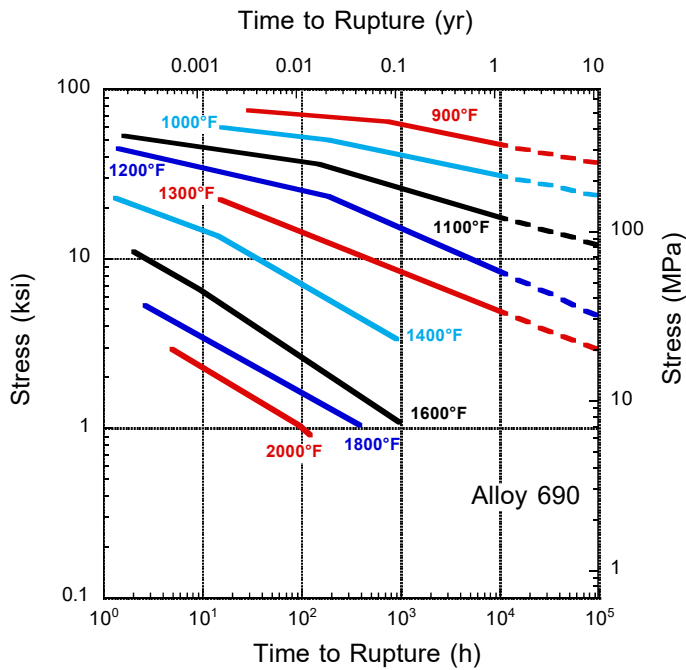


Figure 3. Creep rupture curves of Alloy 690. Dashed lines represent extrapolated data trends.

We used the LMP, defined earlier in Eq. 9, to collapse the data represented by the nine lines at nine temperatures into a single master curve:

$$LMP/1000 = T[C + \log(t_R)] \dots\dots\dots (10)$$

where T is temperature in Kelvin and  $t_R$  is time to rupture in hrs. A best-fit analysis of the data showed that

$$C = 12.14 \dots\dots\dots (11)$$

Figure 4a shows a plot of the test values of the LMP as determined from Eq. (10) and the predicted or fitted values of LMP as determined from Eq. (12).

$$\text{LMP} / 1000 = a_0 + \text{Log}(\text{Stress}) / a_1 \dots\dots\dots(12)$$

Figure 4b shows a plot of the stress vs. LMP parameter. In addition to the mean values, the  $\pm 95$  percent prediction limits are also shown in Figs 4a-b. The equation for the mean value of the LMP is given by (with stress in ksi):

$$\text{Log}_{10}(\text{Stress}) = 4.597 - 0.249(\text{LMP} / 1000) \dots\dots\dots(13)$$

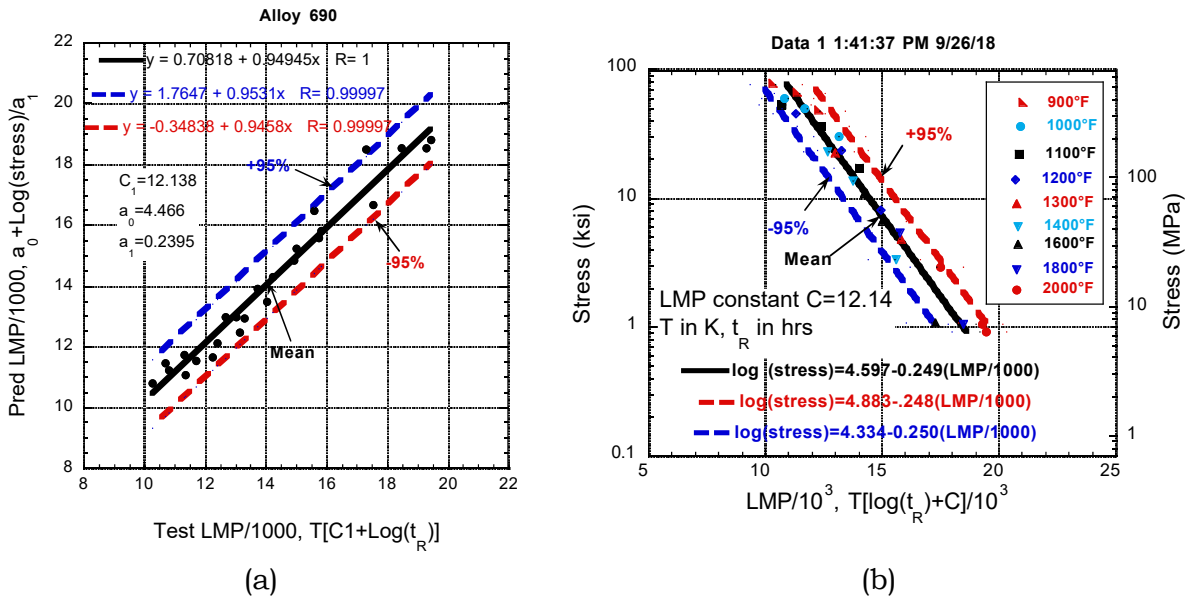


Figure 4. (a) Larson-Miller plot for Alloy 690 creep rupture time data and the (b) observed vs. predicted creep rupture times using the LMP.

The mean and bounding values of the LMP obtained from the plots were used to calculate the predicted times to rupture, which are compared with the test times (as obtained by digitizing Figure 3) in Figure 5. Figure 5 shows that the  $\pm 95$  percent prediction bounds differ from the mean predicted rupture times by a factor of  $\leq 10$ .

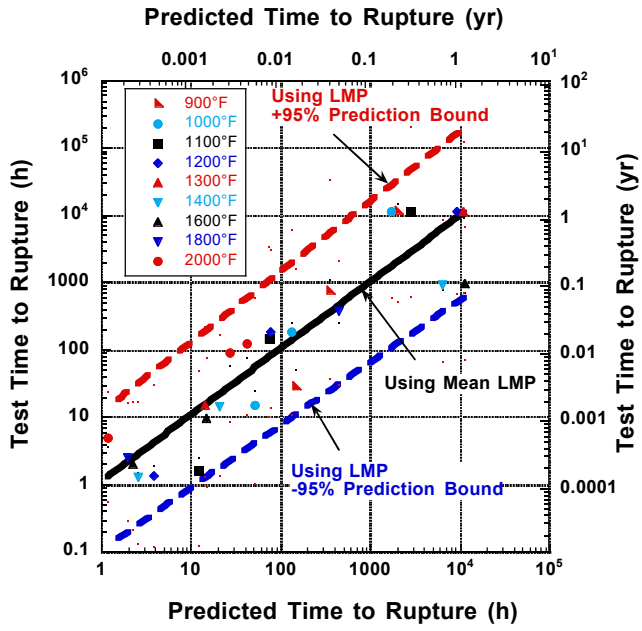


Figure 5. Predicted vs. observed times to rupture of Alloy 690.



### 3. Experimental Basis for Ligament Rupture Pressure, Leak Rate and Unstable Burst Pressure Correlations for SG Tubes with Cracks

#### 3.1 RT Tests

##### 3.1.1 Ligament Rupture and Unstable Burst Pressures

Comparison of predicted and test ligament rupture pressures for 600MA tubes with various PTW notches are given in Figure 6a. A similar plot for unstable burst pressures is shown in Figure 6b. All of these tests were conducted at ANL under the TIP-2 program. Both the test ligament rupture pressures and the test unstable burst pressures are predicted to within their respective  $\pm 95$  percent prediction limits.

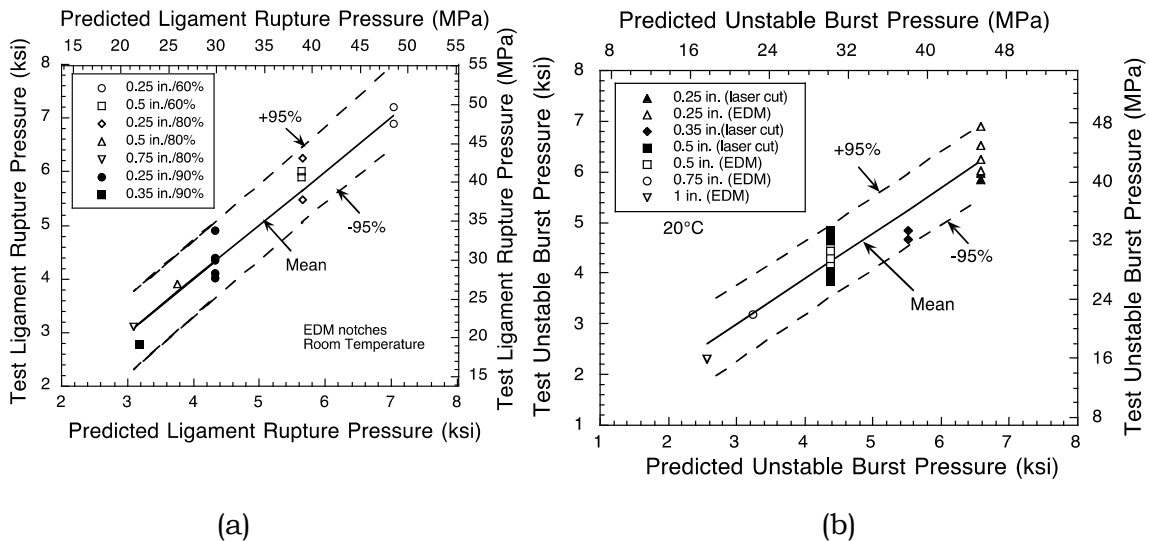
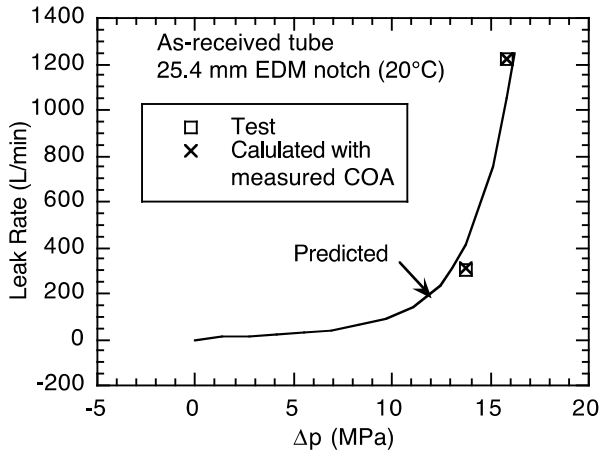


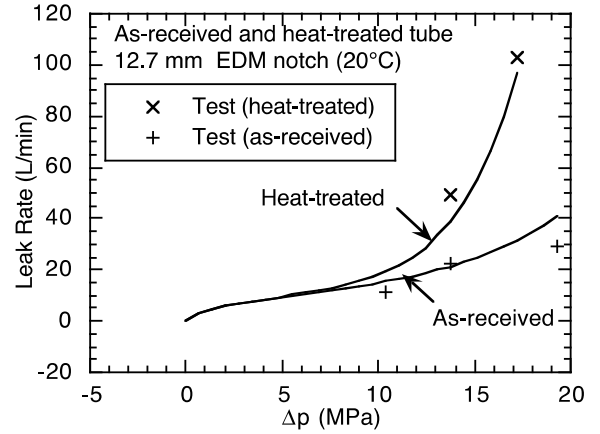
Figure 6. Observed vs. predicted (a) ligament rupture and (b) unstable burst pressures for rectangular EDM notches in 600MA tubes.

##### 3.1.2 Leak Rates

Calculated leak rates for an as-received 600MA tube with a 25 mm (1 in.) EDM notch agree very well with the experimental leak rates, as shown in Figure 7a. Figure 7b shows a similar comparison for 13 mm (0.5 in.) long EDM notches in an as-received tube and in a similar tube but with a high-temperature annealing treatment that reduced its yield strength significantly. As Figure 7b shows, the leak rates in the heat-treated tube, particularly at high pressures, are much greater than those in the as-received tube. Significantly, inclusion of the yield strength change in the predicted leak rate equation can account for the difference in the leak rates between the two tests.



(a)

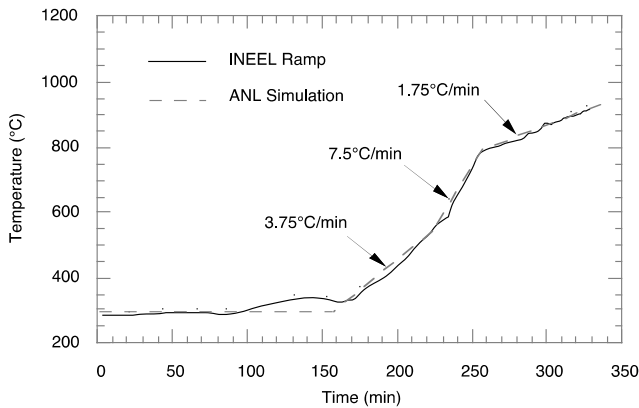


(b)

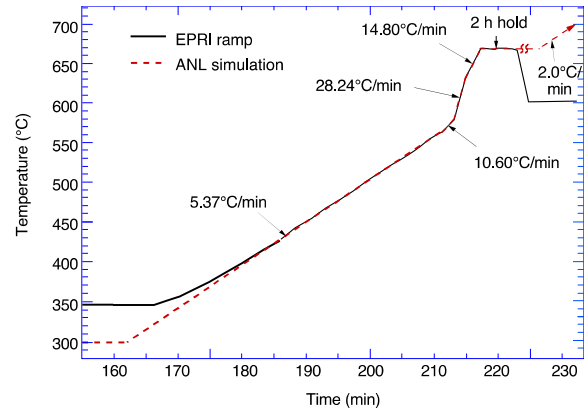
Figure 7. Comparison of calculated (solid line) vs. experimentally measured (symbols) leak rates at 20 °C for as-received and heat-treated 22 mm (0.875 in.) diameter 600MA tubes with (a) 25.4 mm (1 in.) and (b) 12.7 mm (0.5 in.) axial EDM notches. Cross symbols (x) in Figure 7a denote calculated leak rates using posttest measured crack opening areas.

### 3.2 Severe Accident Tests

Simulated severe accident tests were conducted on internally pressurized 600MA tubes at ANL during TIP-2. Two types of analytically derived temperature ramps were available for station blackout severe accidents with the secondary side fully depressurized – Idaho National Engineering and Environmental Laboratory (INEEL) ramp and EPRI ramp.<sup>Error! Reference source not found.,6</sup> In the tests, the analytical ramps were replaced by the piecewise linear approximations shown in Figures 8a-b. The internal pressure was kept constant at 16.2 MPa (2350 psi) while the temperature was ramped.



(a)



(b)

Figure 8. Calculated and ANL simulation of (a) INEEL ramp and (b) EPRI ramp for high-temperature tests.

For predicting creep rupture times of ligaments in PTW cracks due to high temperature and pressure transients, an assumption was made that Eq. 8 was applicable with the stress ( $\sigma$ ) replaced by  $m_p \sigma$ , where  $m_p$  is the ligament stress magnification factor (Eq. 3 a). A number of tests on 600MA tubes with PTW EDM notches were reported in Ref. 2 that justified such an assumption. Plots of the observed vs. predicted failure times and temperatures shown in Figures 9a-b show that the assumption is reasonable for severe accident transients as well.

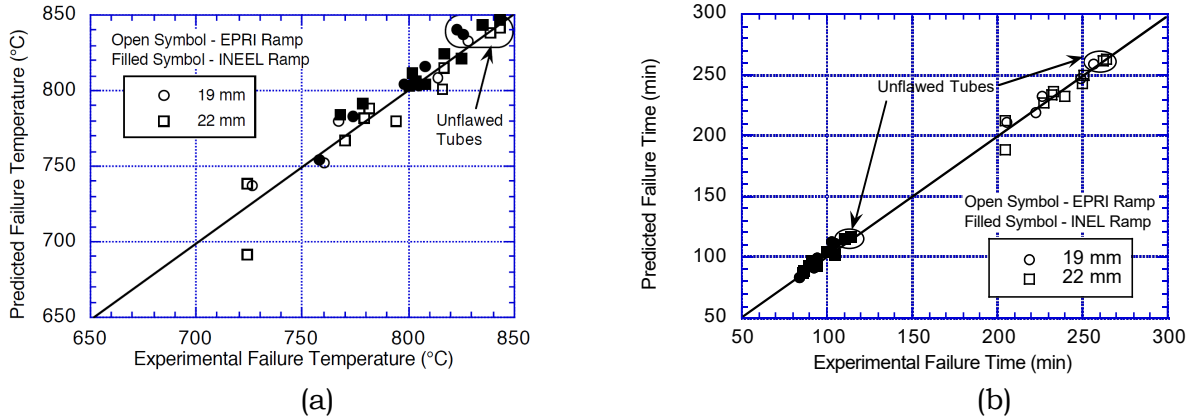


Figure 9. Observed vs. predicted (a) failure temperatures and (b) failure times for tests simulating severe accident transients. Tests were conducted on 19 mm (0.75 in.) as well as 22 mm (0.875 in.) diameter 600MA tubes. Four nominal flaw geometries, with axial lengths of 6 mm (0.25 in.), 25 mm (1 in.), and 50 mm (2 in.) and depths varying from 20 percent to 65 percent of wall thickness, were tested.



## **4. Comparison of Ligament Rupture and Burst Pressures and Leak Rates of 600MA and 690 SG Tubes**

### **4.1 Normal Operation and Design-Basis Accidents**

#### **4.1.1 Ligament Rupture and Burst Pressures**

Table 1 shows that the flow stress (Eq. 1b) of 690TT is 1 percent greater than that of 600MA both at RT and at 650 °F. Equations 4a-b show that, for a given tube size and flaw geometry, both the ligament rupture and the unstable burst pressures are controlled by the flow stress of the material. Therefore, in the absence of test data, our current best estimate is that the ligament rupture and burst pressures of 690TT tubes are on the average 1 percent greater than those of 600MA tubes.

#### **4.1.2 Leak Rate**

Equations 5a-b and 6 show that, for a given crack and differential pressure, the leak rate is controlled by the yield strength of the material. Table 1 shows that the average yield strengths of 600MA and 690TT at 650 °F are equal. Therefore, in the absence of test data, our current best estimate is that the leak rates in 600MA and 690TT tubes for the same-sized cracks and pressure differences are on the average equal.

### **4.2 Severe Accidents**

We used the current base case parameters for the hottest tube as reported by Fletcher and Beaton in ISL-NSAD-TR-06-02 published in March 2006.<sup>7</sup> The pressure and temperature variations in the hottest tubes with time during the base case severe accident transient are plotted in Figure 10. Note that although the pressure differential stays relatively constant, the tube undergoes a rapid increase in temperature rate at ~13,400 seconds.

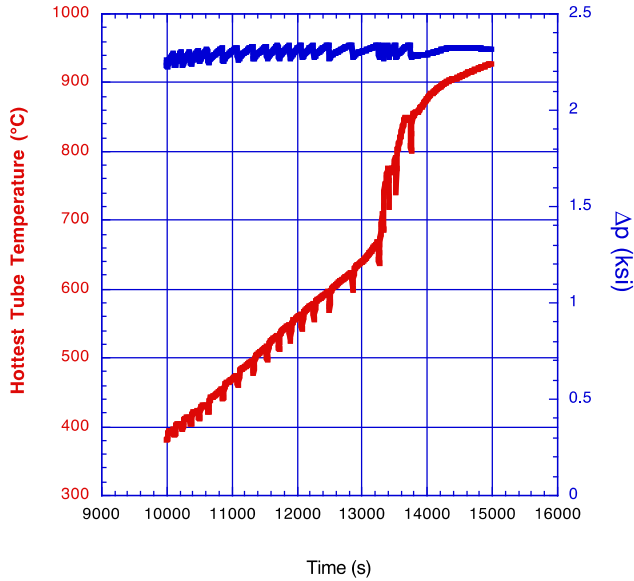
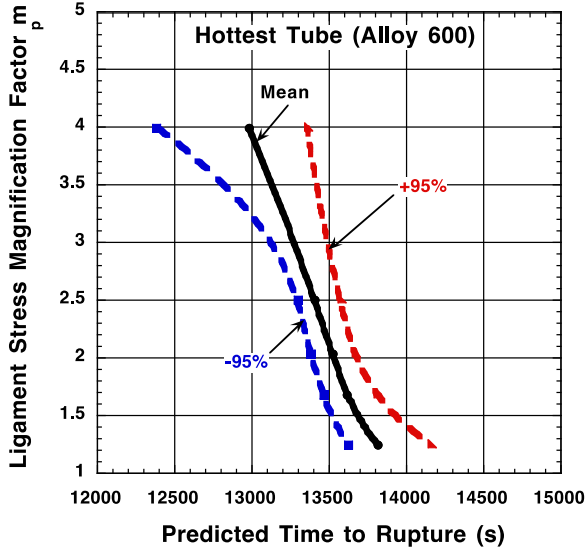


Figure 10. Variations of pressure differential and temperature with time in the hottest SG tubes during the base case scenario.

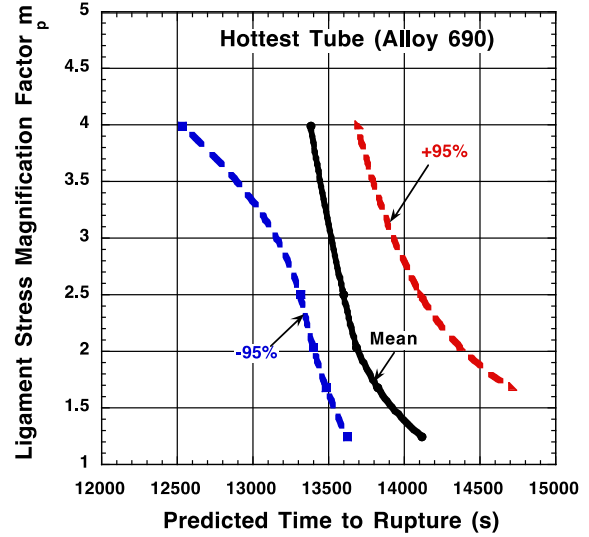
#### 4.2.1 Comparison of Times to Rupture of Alloys 600 and 690 SG Tubes

For the purpose of comparison, the mean and the  $\pm 95$  percent prediction limit curves of the Larson-Miller plots of Alloy 600 were obtained from NUREG/CR-6575 and are reproduced in Figure 2. The Larson-Miller plot for Alloy 690 is given in Figure 4b. The times to rupture of both Alloys 600 and 690 tubes were calculated with the assumption that both were subjected to the same pressure and temperature transients shown in Figure 5.

The rupture times were calculated for PTW axial cracks in 0.875 in. diameter, 0.05 in. wall thickness tubes with an expected range (1.25 to 4) of ligament stress magnification factor,  $m_p$ , in the field. The variations of the mean and  $\pm 95$  percent prediction limits of the time to rupture of Alloys 600 and 690 tubes are plotted against the  $m_p$  factor in Figures 11a-b, respectively. The uncertainty band for the Alloy 690 tubes is greater than that of the 600 tubes because the uncertainty bands of the respective Larson-Miller parameters show a similar trend (Figures 11a and 11b).



(a)



(b)

Figure 11. Variations of mean and  $\pm 95$  percent prediction limits of the times to rupture of Alloys (a) 600 and (b) 690 hottest SG tubes subjected to the base case severe accident transient.

The mean values of the time to rupture of both Alloys are compared in Figure 12. It is evident that, depending on the value of the  $m_p$  factor, the mean values of the time to rupture of 690 tubes exceed those of 600 tubes by between 200-400 seconds.

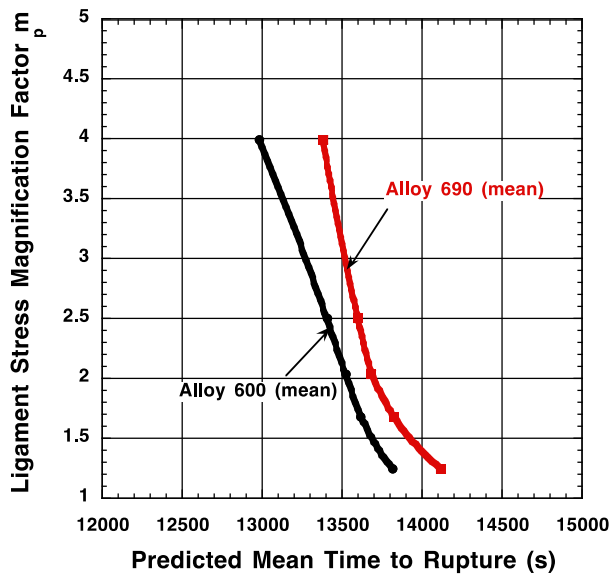


Figure. 12. Comparison of the mean times to rupture of Alloys 600 and 690 tubes subjected to the base case severe accident transient.

## 5. Conclusions

We reviewed the procedures and equations that are used to evaluate structural and leakage integrity of SG tubes under internal pressure and temperature transients. These were originally developed and validated by ANL with pressurized rupture tests on 600MA tubes with flaws. We could not identify or locate similar test data for 690TT tubes with flaws.

We also reviewed the available relevant material properties of 600MA and 690TT tubes that the models use to carry out structural and leakage integrity calculations when the tubes are subjected to loading expected during normal operation, design-basis accident and severe accident. The tensile strength data were analyzed to establish the mean and  $\pm 95$  percent prediction bounds for both materials.

Based on a comparison of the strength data for both materials, we concluded that although there is significant overlap in the data, the mean values of the flow stress of 690TT at RT and at 650 °F are on the average 1 percent higher than those of 600MA at the same temperatures. This observation together with the structural integrity models led us to conclude that, for a given tube size and crack geometry, the mean values of the ligament rupture and unstable burst pressures of 690TT tubes should be 1 percent higher than those of 600MA tubes. Therefore, the structural integrity performance of 690TT tubes, on the average, should be slightly better than that of 600MA tubes during normal operation and design-basis accidents.

The tensile yield strength data of both materials have considerable overlap and the mean values of the yield strength are equal at 650 °F. Together with the leak rate correlations, we conclude that, for a given tube size, crack geometry and pressure difference, the mean values of the leak rate in Alloys 690 TT and 600 TT tubes should be equal. Thus, as far as leakage integrity during normal operation and design-basis accident is concerned, the performance of both materials should be the same.

We computed the times to rupture of Alloys 690 and 600 tubes under the current baseline station blackout severe accident transient on a quasi-statistical basis for a range of crack sizes. Although the uncertainty band for the time to rupture of 690 tube is larger than that of 600 tube, the mean values of the rupture time for 690 tubes are 200-400 seconds greater than those of 600 tubes for the crack sizes considered.

We emphasize that although we are quite confident that the integrity and leakage correlations are robust with respect to their dependence on material properties, all of our calculations for 690TT tubes were conducted without the benefit of a single structural integrity or leakage test on 690TT tube. Therefore, the results presented in this report should be considered as our current best-estimates which will need to be verified by integrity and leakage tests in the future.



## 6. References

1. Saurin Majumdar, Sasan Bakhtiari, Ken Kasza, and Jang Yul Park, "Validation of Failure and Leak Rate Correlations for Stress Corrosion Cracks in SG Tubes", NUREG/CR-6774, 2001.
2. Saurin Majumdar, Ken Kasza and Jeff Franklin, "Failure and Leak Rate Tests and Predictive Models for Flawed SG Tubes," NUREG/CR-6664, 2000.
3. S. Majumdar, W. J. Shack, D. R. Diercks, K. Mruk and J. Franklin, "Failure Behavior of Internally Pressurized Flawed and Unflawed SG Tubing at High Temperatures – Experiments and Comparison with Model Predictions," NUREG/CR-6575, 1998.
4. Publication Number SMC-079, Special Metals Corporation, 2009 (Oct. 09).
5. P. G. Ellison, L. W. Ward, C. A. Dobbe, S. A. Chavez, C. L. Atwood, L. N. Haney, W. G. Reece, and H. S. Blackman, SG Induced Rupture from Operating Transients, Design-Basis Accidents, and Severe Accidents, INEL-95/0641, Idaho National Engineering Laboratory, Aug. 1996.
6. E. L. Fuller, M. A. Kenton, M. Epstein, R. E. Henry, and N. G. Cofie, Risks from Severe Accidents Involving SG Tube Leaks or Ruptures, EPRI TR-106194, Electric Power Research Institute, Palo Alto, CA, 1996.
7. C.D. Fletcher and R. M. Beaton, "SCDAP/RELAP5 Base Case Calculations for the Zion Station Blackout Uncertainty Study," ISL-NSAD\_TR-06-02, Information Systems Laboratories Inc., Idaho Falls, Idaho, Report Prepared for Office of Nuclear Regulatory Research, USNRC, March 2006.